

# Photoelectron spectroscopy and density functional theory study of $\text{TiAlO}_y^-$ ( $y=1-3$ ) and $\text{TiAl}_2\text{O}_y^-$ ( $y=2-3$ ) clusters

Zeng-Guang Zhang, Hong-Guang Xu, Yuchao Zhao, and Weijun Zheng<sup>a)</sup>

Beijing National Laboratory for Molecular Science, State Key Laboratory of Molecular Reaction Dynamics, Institute of Chemistry, Chinese Academy of Sciences, Beijing 100190, China

(Received 6 July 2010; accepted 5 October 2010; published online 20 October 2010)

Small titanium-aluminum oxide clusters,  $\text{TiAlO}_y^-$  ( $y=1-3$ ) and  $\text{TiAl}_2\text{O}_y^-$  ( $y=2-3$ ), were studied by using anion photoelectron spectroscopy. The adiabatic detachment energies of  $\text{TiAlO}_y^-$  ( $y=1-3$ ) were estimated to be  $1.11 \pm 0.05$ ,  $1.70 \pm 0.08$ , and  $2.47 \pm 0.08$  eV based on their photoelectron spectra; those of  $\text{TiAl}_2\text{O}_2^-$  and  $\text{TiAl}_2\text{O}_3^-$  were estimated to be  $1.17 \pm 0.08$  and  $2.2 \pm 0.1$  eV, respectively. The structures of these clusters were determined by comparison of density functional calculations with the experimental results. The structure of  $\text{TiAlO}^-$  is nearly linear with the O atom in the middle. That of  $\text{TiAlO}_2^-$  is a kite-shaped structure.  $\text{TiAlO}_3^-$  has a kite-shaped  $\text{TiAlO}_2$  unit with the third O atom attaching to the Ti atom.  $\text{TiAl}_2\text{O}_2^-$  has two nearly degenerate Al–O–Ti–O–Al chain structures that can be considered as *cis* and *trans* forms.  $\text{TiAl}_2\text{O}_3^-$  has two low-lying isomers, kite structure and book structure. The structures of these clusters indicate that the Ti atom tends to bind to more O atoms. © 2010 American Institute of Physics. [doi:10.1063/1.3505298]

## I. INTRODUCTION

Since titanium oxides and aluminum oxides have broad applications in the fields of catalysis and microelectronics, many experimental and theoretical works have been devoted to investigating their structures and properties. The titanium oxide and aluminum oxide clusters have attracted special attention because they serve as simple models for tracking the evolution of the properties of these oxides from the microscale to the macroscale. Experimentally, titanium oxide clusters of different stoichiometries were studied with mass spectrometry,<sup>1,2</sup> matrix isolation experiments,<sup>3-5</sup> negative ion photoelectron spectroscopy,<sup>6,7</sup> photofragment experiments,<sup>8</sup> and Fourier transform microwave spectroscopy.<sup>9</sup> Aluminum oxygen clusters were also investigated with negative ion photoelectron spectroscopy,<sup>10-16</sup> matrix isolation experiments,<sup>17-19</sup> and infrared predissociation spectroscopy.<sup>20</sup> The titanium oxide and aluminum oxide clusters were studied with infrared resonance enhanced multiphoton ionization spectroscopy<sup>21</sup> as well. Theoretically, a number of methods were employed to explore the structures and bonding of the clusters of titanium<sup>22-37</sup> and aluminum oxides.<sup>38-53</sup>

Although the clusters of titanium oxide and aluminum oxide were intensively investigated, the study of hybrid titanium-aluminum oxides is quite rare. In the past few years, it has been proposed that hybrid titanium-aluminum oxides might have potential applications as a high-dielectric (high-K) material for the next generation of complementary metal-oxide-semiconductor (CMOS) gates.<sup>54,55</sup> It was also suggested that TiAlO films of different thickness may be used as high-reflection or antireflection layers for solar

cells.<sup>56</sup> Very recently, the comparison of experimental data and astronomical observations implies that titanium-aluminum oxides, such as  $\text{TiAlO}_3$  and  $\text{TiAl}_2\text{O}_5$ , might contribute to the infrared spectra of asymptotic giant branch stars.<sup>57</sup> Therefore, understanding the structures and properties of titanium-aluminum oxides is important from both technological and scientific points of view. With this motivation, we conducted a combined photoelectron spectroscopy and density functional theory study of the structures and electronic properties of small  $\text{TiAl}_x\text{O}_y^-$  ( $x=1,2$ ;  $y=1-3$ ) clusters.

## II. EXPERIMENTAL AND THEORETICAL METHODS

### A. Experimental

The experiments were performed using a home-built apparatus consisting of a laser vaporization source, a time-of-flight (TOF) mass spectrometer, and a magnetic-bottle photoelectron spectrometer.<sup>58</sup> The details of our apparatus have been described elsewhere.<sup>59</sup> Briefly, a rotating and translating disk target of Al/Ti mixture (Al/Ti mole ratio 10:1) was ablated with a pulsed laser beam (10 mJ/pulse at 532 nm) from a nanosecond Nd:YAG (yttrium aluminum garnet) laser. The laser-induced plasma was mixed with helium carrier gas that was allowed to expand into the source through a pulsed valve at  $\sim 4$  atm backing pressure. The presence of  $\text{TiAl}_x\text{O}_y^-$  clusters arose from a small amount of oxygen in the carrier gas and on the surface of the target. After a supersonic expansion, the cluster anions formed were collimated by a skimmer, perpendicularly extracted to their flow direction by a pulsed electric field and then mass analyzed by the TOF mass spectrometer. The mass peaks of  $\text{TiAl}_x\text{O}_y^-$  clusters were confirmed by the isotope distributions and by running control experiments with pure aluminum target. The

<sup>a)</sup> Author to whom correspondence should be addressed. Electronic mail: zhengwj@iccas.ac.cn. Tel.: +86 10 62635054. FAX: +86 10 62563167.

anions of interest were selected with a mass gate and decelerated before photodetachment by a second laser beam (532 or 266 nm). The kinetic energies of the electrons were measured using a magnetic-bottle photoelectron analyzer. The electron binding energies were obtained via equation:  $EBE = hv - EKE$ , where EBE is the electron binding energy,  $hv$  is the photon energy, and EKE is the electron kinetic energy. The photoelectron spectra were calibrated with known spectra of  $Cu^-$  and  $Au^-$ .

## B. Theoretical methods

Computations were performed with the GAUSSIAN 03 package<sup>60</sup> using the B3LYP (Becke 3-parameter-Lee-Yang-Parr)<sup>61,62</sup> density functional method. The 6-311+G(2d) basis sets were used for Al and O atoms, and the LanL2DZ basis set was employed for Ti atoms. We tested the theoretical method by calculating the bond lengths and electron affinities of AlO and TiO. The calculations show that the bond lengths of AlO and TiO are 1.631 and 1.615 Å, respectively, in agreement with the experimental values (1.618 Å for AlO and 1.620 Å for TiO) (Ref. 63) reported in the literature. The electron affinities of AlO and TiO were calculated to be 2.54 and 1.15 eV, respectively, also close to the experimental values [(2.60 eV for AlO (Ref. 10) and 1.30 eV for TiO (Ref. 6)]. That indicates that the B3LYP density function method with the mixed basis set of 6-311+g(2d) and LanL2DZ is suitable for the calculation of  $TiAl_xO_y^-$  clusters. We conducted calculations on  $TiAl_xO_y^-$  ( $x=1-2$ ;  $y=1-3$ ) clusters as well as their corresponding neutral with all possible candidate isomers. Full geometrical optimization was performed at various possible spin multiplicities in order to find the global minimum for each species. Harmonic vibrational frequency analysis was performed to verify the nature of the stationary points. All calculated energies were corrected by the zero-point vibrational energies. The natural population analysis for the  $TiAl_xO_y$  clusters was performed as implemented in the GAUSSIAN 03 program.<sup>64</sup>

## III. EXPERIMENTAL RESULTS

The photoelectron spectra of the  $TiAlO_y^-$  ( $y=1-3$ ) and  $TiAl_2O_y^-$  ( $y=2-3$ ) cluster anions taken with 266 nm (4.661 eV) photons are shown in Fig. 1. The adiabatic detachment energies (ADEs) and vertical detachment energies (VDEs) of these clusters estimated from their photoelectron spectra are summarized in Table I. The VDEs were determined as the positions of the first photoelectron spectrum peaks. To account for the broadening of the photoelectron spectral peaks due to instrumental resolution, the adiabatic detachment energies were calculated by adding half of the value of instrumental resolution to the onset of the first peaks in the spectra.

In the photoelectron spectrum of  $TiAlO^-$  taken with 266 nm photons, we observed two major peaks centered at 1.11 and 1.69 eV. There are also some weak features on the higher binding energy side of the spectrum, which cannot be resolved due to the poor signal-to-noise ratio. To investigate  $TiAlO^-$  in detail, we also took the spectrum of  $TiAlO^-$  with 532 nm photons and present it in Fig. 2. We can see that the relative intensities of the two major features of  $TiAlO^-$  in the

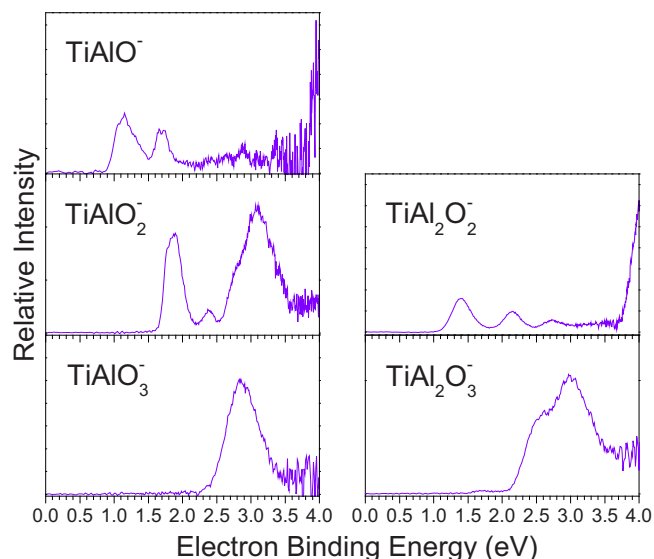


FIG. 1. Photoelectron spectra of  $TiAlO_y^-$  ( $y=1-3$ ) and  $TiAl_2O_y^-$  ( $y=2-3$ ) clusters recorded with 266 nm photons.

532 and 266 nm spectra are different. That probably is owing to the wavelength dependence of photodetachment cross section. The spectrum taken with 532 nm photons gives better resolution than the spectrum at 266 nm. In Fig. 2, two major peaks are observed at 1.11 and 1.67 eV, respectively, corresponding to the transitions from the ground state of  $TiAlO^-$  to the ground state and the first electronic excited state of  $TiAlO$  neutral. The ADE and VDE of  $TiAlO^-$  are estimated to be 1.11 and 1.11 eV. We can also observe some small peaks behind these major peaks at 1.21, 1.32, and 1.77 eV. These small peaks probably are due to the vibrations of  $TiAlO$  neutral. We estimated the vibration frequency to be  $810 \pm 80 \text{ cm}^{-1}$  based on the spacing between the small peaks.

The spectrum of  $TiAlO_2^-$  reveals an intense feature centered at 1.87 eV, followed by a small peak centered at 2.38 eV and a broad feature at 3.10 eV. A more detailed spectrum of  $TiAlO_2^-$  taken at 532 nm (Fig. 2) shows a different shape for the first feature, indicating that feature is probably composed of a few unresolved vibrational structures. Based on the 532 nm spectrum, the VDE of  $TiAlO_2^-$  is determined to be 1.79 eV. In the spectrum of  $TiAlO_3^-$ , one can only observe a broad feature at 2.84 eV. The spectrum of  $TiAl_2O_2^-$  has three peaks centered at 1.40, 2.15, and 2.73 eV with

TABLE I. Vertical detachment energies and adiabatic detachment energies of  $TiAlO_y^-$  ( $y=1-3$ ) and  $TiAl_2O_y^-$  ( $y=2-3$ ) estimated from their photoelectron spectra.

Cluster	VDE (eV) <sup>a</sup>	ADE (eV) <sup>a</sup>
$TiAlO^-$	1.11(5) <sup>b</sup>	1.11(5) <sup>b</sup>
$TiAlO_2^-$	1.79(8) <sup>b</sup>	1.70(8) <sup>b</sup>
$TiAlO_3^-$	2.84(8)	2.47(8)
$TiAl_2O_2^-$	1.40(8)	1.17(8)
$TiAl_2O_3^-$	2.6(1)	2.2(1)

<sup>a</sup>The numbers in parentheses indicate the uncertainties in the last digit.

<sup>b</sup>Measured at 532 nm.

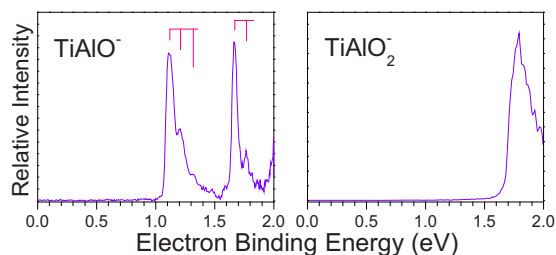


FIG. 2. Photoelectron spectra of  $\text{TiAlO}^-$  and  $\text{TiAlO}_2^-$  clusters recorded with 532 nm photons. The vertical lines point to the vibrational structures.

gradually decreasing intensities, and an additional strong feature is observed beyond 3.8 eV. The spectrum of  $\text{TiAl}_2\text{O}_3^-$  shows a very broad feature between 2.1 and 3.6 eV, which is composed of two unresolved peaks centered at 2.6 and 3.0 eV, respectively.

#### IV. THEORETICAL RESULTS AND DISCUSSION

To investigate the structures and properties of  $\text{TiAl}_x\text{O}_y^-$  clusters, we conducted density functional calculations on these clusters and their neutrals. The optimized geometries of the low-lying isomers of  $\text{TiAlO}_y^-$  ( $y=1-3$ ) and  $\text{TiAl}_2\text{O}_y^-$  ( $y=2-3$ ) clusters are presented in Fig. 3 with the most stable isomers on the left. For comparison, the calculated relative energies, ADEs and VDEs of the low-lying isomers are summarized in Table II along with the experimental ADEs and VDEs. The theoretical vertical electron detachment energies were calculated as the energy differences between the anions and neutrals at the geometries of the anions. The theoretical adiabatic electron detachment energies were calculated as the energy differences between the anions and the neutrals relaxed to the nearest local minima using the geometries of the

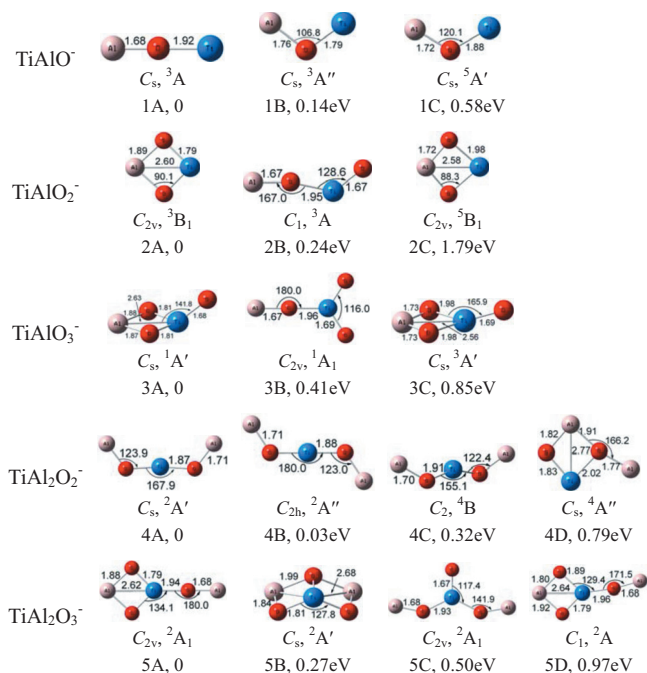


FIG. 3. Structures and relative energies of the low-lying isomers of  $\text{TiAlO}_{1-3}^-$  and  $\text{TiAl}_2\text{O}_{2-3}^-$  cluster anions. The Al, O, and Ti atoms are shown in light purple, red, and blue, respectively. The bond distances are in angstrom and the bond angles are in degrees.

anions as initial structures. The structures of low-lying isomers of  $\text{TiAl}_x\text{O}_y$  neutrals are shown in Fig. 4.

##### A. $\text{TiAlO}^-$

The most stable structure of  $\text{TiAlO}^-$  (1A) is nearly linear ( $\angle \text{AlOTi} = 179.8^\circ$ ) with the O atom locating in the middle of the Al and Ti atoms. We have tried to confine the structure of

TABLE II. The calculated symmetry, multiplicity, relative energy, ADEs and VDEs of the low-lying isomers of  $\text{TiAlO}_y^-$  ( $y=1-3$ ) and  $\text{TiAl}_2\text{O}_y^-$  ( $y=2-3$ ) clusters as well as the comparison between experimental and theoretical results.

Cluster	Symmetry	Multiplicity	$\Delta E$ (eV)	ADE (eV)		VDE (eV)		
				Theor.	Expt.	Theor.	Expt.	
$\text{TiAlO}^-$	(1A)	$C_s$	3	0	0.88	1.11	0.93	1.11
	(1B)	$C_s$	3	0.14	0.74		1.03	
	(1C)	$C_s$	5	0.58	0.29		0.47	
$\text{TiAlO}_2^-$	(2A)	$C_{2v}$	3	0	1.42	1.70	1.57	1.79
	(2B)	$C_1$	3	0.24	1.38		1.47	
	(2C)	$C_{2v}$	5	1.79	0.44		0.66	
$\text{TiAlO}_3^-$	(3A)	$C_s$	1	0	2.51	2.47	2.91	2.84
	(3B)	$C_{2v}$	1	0.41	3.72		3.92	
	(3C)	$C_s$	3	0.85	1.65		2.31	
$\text{TiAl}_2\text{O}_2^-$	(4A)	$C_s$	2	0	1.01	1.17	1.33	1.40
	(4B)	$C_{2h}$	2	0.03	0.99		1.34	
	(4C)	$C_2$	4	0.32	0.69		1.17	
	(4D)	$C_s$	4	0.79	0.22		1.38	
$\text{TiAl}_2\text{O}_3^-$	(5A)	$C_{2v}$	2	0	2.21	2.2	2.89	2.6
	(5B)	$C_s$	2	0.27	2.20		2.50	
	(5C)	$C_{2v}$	2	0.50	1.75		2.13	
	(5D)	$C_1$	2	0.97	1.51		1.90	

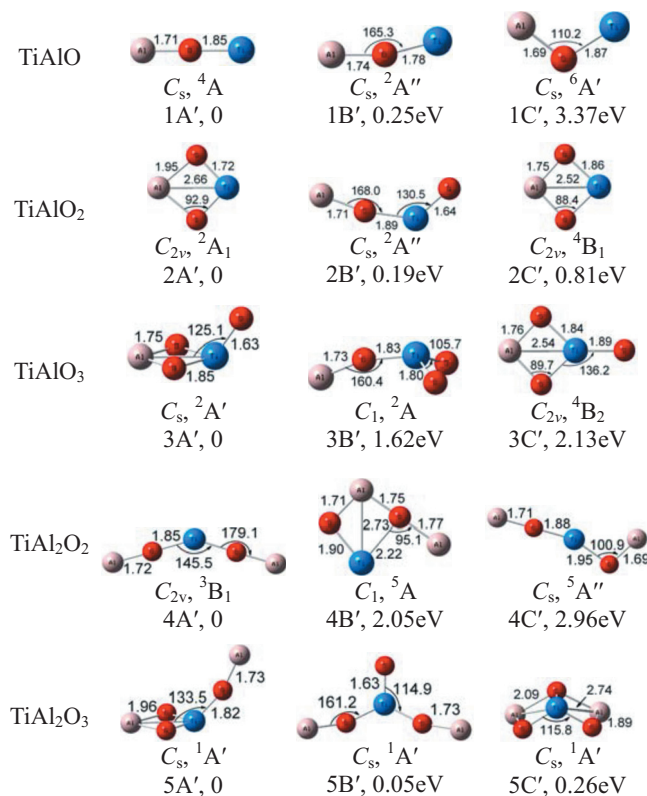


FIG. 4. Structures and relative energies of the low-lying isomers of neutral  $TiAlO_{1-3}$  and  $TiAl_2O_{2-3}$  clusters. The Al, O, and Ti atoms are shown in light purple, red, and blue, respectively. The bond distances are in angstrom and the bond angles are in degrees.

$TiAlO^-$  to  $C_{\infty v}$  symmetry but found an imaginary frequency. That implies that the structure of  $TiAlO^-$  is not perfectly linear. Isomers 1B and 1C have bent structures also with the O atom in the middle. Isomer 1B is higher than isomer 1A by 0.14 eV. Isomer 1C is higher than isomer 1A by 0.58 eV. The calculated ADE and VDE of isomer 1C are very different from our experiment values. Therefore, the existence of isomer 1C in the experiments can be excluded. The VDE and ADE of isomer 1B are calculated to be 1.03 and 0.74 eV, respectively. The difference between the VDE and ADE is about 0.3 eV, indicating there is a significant geometry change between isomer 1B and its corresponding neutral. However, in our experimental results (Fig. 2), the first photoelectron spectrum peak is quite sharp, which means the geometry displacement between the anion and neutral is relatively small. Thus, the existence of isomer 1B in the experiments can also be excluded. The ADE and VDE of isomer 1A are calculated to be 0.88 and 0.93 eV in reasonable agreement with the experiment values. We suggest that isomer 1A is the most possible isomer observed in the experiments. Our calculations found that the most stable structure of  $TiAlO$  neutral is also nearly linear, very similar to the  $D_{\infty h}$  symmetry linear structure of  $Al_2O$  obtained by theoretical calculations.<sup>49,65</sup> The frequency of the antisymmetric stretching mode of  $TiAlO$  neutral is calculated to be  $890\text{ cm}^{-1}$  after a scale factor of 0.96. That is in agreement with the vibrational structure ( $810 \pm 80\text{ cm}^{-1}$ ) observed in our experiments (Fig. 2). Theoretical calculations of Jeong *et al.*<sup>30</sup>

found  $Ti_2O$  to be a bent structure. The second stable isomer of  $TiAlO$  neutral is analogous to the structure of  $Ti_2O$ .

## B. $TiAlO_2^-$

The most stable structure of  $TiAlO_2^-$  is isomer 2A. It is a  $C_{2v}$  symmetry kite shape structure with two bridging oxygen atoms. The ADE and VDE of isomer 2A are calculated to be 1.42 and 1.57 eV in agreement with our experiment. Isomer 2B is 0.24 eV higher than isomer 2A in energy. It is a bent chain structure arranged in the order of Al–O–Ti–O. Its ADE and VDE (1.38 and 1.47 eV) are slightly off from the experimental values. Isomer 2C is also a kite style planar structure with  $C_{2v}$  symmetry similar to isomer 2A except the Al–O bonds (1.72 Å) in isomer 2C are shorter than the Ti–O bonds (1.98 Å) in contrast to those in isomer 2A. Isomer 2C is less stable than isomer 2A by 1.79 eV. Its ADE and VDE are very different from the experimental values. Thus, the existence of isomer 2C in the experiment can be ruled out. We suggest isomer 2A to be the most possible isomer observed in the experiments. Our calculations show that the most stable structure of  $TiAlO_2$  neutral is also kite shape. That is somewhat in agreement with the rhombus structures of  $Al_2O_2$  (Refs. 49, 51, and 65) and  $Ti_2O_2$  (Ref. 30) reported in the literature, except replacing one of the metal atoms in  $Al_2O_2$  or  $Ti_2O_2$  alternates the rhombus to kite.

## C. $TiAlO_3^-$

The most stable structure of  $TiAlO_3^-$  (isomer 3A) has a kite-shaped  $TiAlO_2$  unit with the third O atom attaching to the Ti atom. The third O atom bends away from the plane of the kite. The ADE and VDE of isomer 3A are calculated to be 2.51 and 2.91 eV, in good agreement the experiment measurements. Isomer 3B and 3C are less stable than isomer 3A by 0.41 and 0.85 eV, respectively. Their ADEs and VDEs are different from the experimental measurement. Thus, the existence of isomer 3B and 3C in our experiments can be excluded. Isomer 3A probably is what we observed in the experiment. The most stable structure of  $TiAlO_3$  neutral is also calculated to be kite. It is interesting to compare the structure of  $TiAlO_3$  with those of  $Ti_2O_3$  and  $Al_2O_3$ . Jeong *et al.*<sup>30</sup> found that  $Ti_2O_3$  has a kite structure with the third O atom bending away from the plane of the kite. As for  $Al_2O_3$ , its most stable structure has been found to be linear O–Al–O–Al–O with  $D_{\infty h}$  symmetry, its second stable structure has been found to be  $C_{2v}$  symmetry kite structure with the third O atom coplanar with the  $Al_2O_2$  unit.<sup>65</sup> We have tried to look for the O–Al–O–Ti–O linear and chain structures. However, we found these geometries are unstable, which probably is because the Ti atom tends to bond to more O atoms. The geometry of  $TiAlO_3$  is more similar to the geometry of  $Ti_2O_3$  than that of  $Al_2O_3$  since the third O atom in  $TiAlO_3$  attaches to the Ti atom instead of the Al atom.

## D. $TiAl_2O_2^-$

The lowest two isomers (4A, and 4B) of  $TiAl_2O_2^-$  are nearly degenerate in energy. Isomer 4B is only 0.03 eV higher than isomer 4A. Both isomer 4A and 4B are bent

chain structures arranged in the order of Al–O–Ti–O–Al. They are bent toward different directions, so that isomer 4A can be considered as a *cis* structure and isomer 4B as a *trans* structure. Note, in isomer 4A, the Ti atom is slightly above the plane determined by the other four atoms. The Al–O and Ti–O bond lengths in these two isomers are almost same. It has been reported that the ground state of  $\text{Al}_3\text{O}_2^-$  possesses a kite structure with the third Al atom bonding to one of two bridged oxygen.<sup>51</sup> For  $\text{TiAl}_2\text{O}_2^-$ , however, this kite geometry is less stable than the chain structures. Our calculations found a few higher energy isomers for  $\text{TiAl}_2\text{O}_2^-$  anion, such as 4C and 4D. The ADEs and VDEs of those high energy isomers are not in agreement with the experimental values. As a result, the existence of isomers 4C and 4D in the experiment can be ruled out. The computed ADEs and VDEs of 4A and 4B fit well with the experimental values. Hence, we suggest that both isomer 4A and 4B exist in our experiments. The  $\text{TiAl}_2\text{O}_2$  neutral has a V-shape structure arranged in the order of Al–O–Ti–O–Al, which is similar to the V-shape structure of  $\text{Al}_3\text{O}_2$ .<sup>42,47,51</sup> Our calculations show that the kite structure of  $\text{TiAl}_2\text{O}_2$  is less stable than the V-shape structure by 2.05 eV. No *trans* isomer has been found for  $\text{TiAl}_2\text{O}_2$  neutral.

### E. $\text{TiAl}_2\text{O}_3^-$

The most stable isomer (5A) of  $\text{TiAl}_2\text{O}_3^-$  has a  $C_{2v}$  symmetric planar structure with a kite-shaped  $\text{TiAlO}_2$  unit and an O–Al bond tail, which is similar to the kite structure of  $\text{Al}_3\text{O}_3^-$ .<sup>11,42,46,47</sup> This configuration is based on isomer 3A of  $\text{TiAlO}_3^-$  by adding an extra Al to the terminal oxygen atom.

Isomer 5B lies 0.27 eV above isomer 5A. It is a book structure, which is also similar to the book structure of  $\text{Al}_3\text{O}_3^-$  (Refs. 42, 46, and 47) and  $\text{Ti}_3\text{O}_3$ .<sup>30</sup> The book structure (5B) can be considered as two kites merged together via the Ti–O edge. The computed ADEs and VDEs of 5A and 5B coincide with the experimental values as revealed in Table II. It might be possible that both isomer 5A and 5B were populated in the photoelectron spectroscopy experiments. We found that the most stable structure of  $\text{TiAl}_2\text{O}_3$  neutral is also kite, similar to that of the anion although its O–Al bond tail bends away from the plane. That is slightly different from the case of  $\text{Al}_3\text{O}_3$  and  $\text{Al}_3\text{O}_3^-$ , whereas the most stable structures for the anion and neutral are different, the kite structure is more stable for  $\text{Al}_3\text{O}_3$  while the book structure is more stable for  $\text{Al}_3\text{O}_3^-$ .<sup>42,45,47</sup> In addition to the kite and book structures, we also found anchor structures for  $\text{TiAl}_2\text{O}_3$  neutral (Fig. 4, 5B') and anion (Fig. 3, 5C). The anchor structure of  $\text{TiAl}_2\text{O}_3$  neutral is even more stable than the book structure. However, for the anion, the anchor structure is less stable than the book structure, its ADE and VDE is different from the experimental measurements. The anchor structure probably is not what we observed in the experiments.

As it can be seen from the structures in Fig. 3 and 4, the Ti atom tends to bind to more O atoms than the Al atom, which is consistent with the fact that the dissociation energy of Ti–O ( $6.92 \pm 0.1$  eV) is bigger than that of Al–O ( $5.26 \pm 0.1$  eV).<sup>66</sup> Our calculations show that, for both  $\text{TiAlO}_y$  and  $\text{TiAl}_2\text{O}_y$ , the electron affinities increase as the number of O atoms increases in the clusters. The electron affinity of  $\text{TiAl}_2\text{O}_y$  is relatively lower than that of  $\text{TiAlO}_y$

TABLE III. Natural populations and natural electron configurations of the most stable isomers of  $\text{TiAlO}_y^-$  ( $y=1-3$ ) and  $\text{TiAl}_2\text{O}_y^-$  ( $y=2-3$ ) clusters and their corresponding neutrals at the B3LYP level.

Cluster	Atom	Natural electron configuration		Natural charge	
		Anion	Neutral	Anion	Neutral
$\text{TiAlO}$ (1A)	O	[Core]2s <sup>1.90</sup> 2p <sup>5.62</sup>	[Core]2s <sup>1.90</sup> 2p <sup>5.60</sup>	−1.58	−1.55
	Ti	[Core]4s <sup>1.83</sup> 3d <sup>2.23</sup>	[Core]4s <sup>0.88</sup> 3d <sup>2.35</sup>	−0.12	0.74
	Al	[Core]3s <sup>1.78</sup> 3p <sup>0.51</sup>	[Core]3s <sup>1.83</sup> 3p <sup>0.35</sup>	0.69	0.81
$\text{TiAlO}_2$ (2A)	O(1)	[Core]2s <sup>1.89</sup> 2p <sup>5.34</sup>	[Core]2s <sup>1.89</sup> 2p <sup>5.16</sup>	−1.25	−1.07
	O(2)	[Core]2s <sup>1.89</sup> 2p <sup>5.34</sup>	[Core]2s <sup>1.89</sup> 2p <sup>5.16</sup>	−1.25	−1.07
	Ti	[Core]4s <sup>0.77</sup> 3d <sup>2.31</sup>	[Core]4s <sup>0.40</sup> 3d <sup>2.26</sup>	0.83	1.34
	Al	[Core]3s <sup>1.67</sup> 3p <sup>0.62</sup>	[Core]3s <sup>1.76</sup> 3p <sup>0.40</sup>	0.67	0.80
	Al	[Core]3s <sup>1.67</sup> 3p <sup>0.62</sup>	[Core]3s <sup>1.76</sup> 3p <sup>0.40</sup>	0.67	0.80
$\text{TiAlO}_3$ (3A)	O(1)	[Core]2s <sup>1.87</sup> 2p <sup>5.31</sup>	[Core]2s <sup>1.86</sup> 2p <sup>5.32</sup>	−1.20	−1.21
	O(2)	[Core]2s <sup>1.87</sup> 2p <sup>5.31</sup>	[Core]2s <sup>1.86</sup> 2p <sup>5.32</sup>	−1.20	−1.21
	O(3)	[Core]2s <sup>1.90</sup> 2p <sup>5.02</sup>	[Core]2s <sup>1.91</sup> 2p <sup>4.83</sup>	−0.96	−0.76
	Ti	[Core]4s <sup>0.09</sup> 3d <sup>2.20</sup>	[Core]4s <sup>0.09</sup> 3d <sup>2.17</sup>	1.68	1.73
	Al	[Core]3s <sup>1.71</sup> 3p <sup>0.59</sup>	[Core]3s <sup>0.91</sup> 3p <sup>0.60</sup>	0.67	1.45
$\text{TiAl}_2\text{O}_2$ (4A)	O(1)	[Core]2s <sup>1.87</sup> 2p <sup>5.53</sup>	[Core]2s <sup>1.89</sup> 2p <sup>5.57</sup>	−1.42	−1.48
	O(2)	[Core]2s <sup>1.87</sup> 2p <sup>5.53</sup>	[Core]2s <sup>1.89</sup> 2p <sup>5.57</sup>	−1.42	−1.48
	Ti	[Core]4s <sup>0.99</sup> 3d <sup>2.26</sup>	[Core]4s <sup>0.53</sup> 3d <sup>2.17</sup>	0.72	1.28
	Al(1)	[Core]3s <sup>1.79</sup> 3p <sup>0.62</sup>	[Core]3s <sup>1.84</sup> 3p <sup>0.31</sup>	0.57	0.84
	Al(2)	[Core]3s <sup>1.79</sup> 3p <sup>0.62</sup>	[Core]3s <sup>1.84</sup> 3p <sup>0.31</sup>	0.57	0.84
$\text{TiAl}_2\text{O}_3$ (5A)	O(1)	[Core]2s <sup>1.86</sup> 2p <sup>5.30</sup>	[Core]2s <sup>1.88</sup> 2p <sup>5.14</sup>	−1.18	−1.04
	O(2)	[Core]2s <sup>1.86</sup> 2p <sup>5.30</sup>	[Core]2s <sup>1.88</sup> 2p <sup>5.14</sup>	−1.18	−1.03
	O(3)	[Core]2s <sup>1.86</sup> 2p <sup>5.60</sup>	[Core]2s <sup>1.87</sup> 2p <sup>5.48</sup>	−1.48	−1.38
	Ti	[Core]4s <sup>0.28</sup> 3d <sup>2.27</sup>	[Core]4s <sup>0.09</sup> 3d <sup>2.11</sup>	1.42	1.79
	Al(1)	[Core]3s <sup>1.70</sup> 3p <sup>0.59</sup>	[Core]3s <sup>1.79</sup> 3p <sup>0.39</sup>	0.68	0.81
	Al(2)	[Core]3s <sup>1.81</sup> 3p <sup>0.42</sup>	[Core]3s <sup>1.85</sup> 3p <sup>0.28</sup>	0.75	0.85

( $y=2-3$ ) with the same number O atoms. This trend is in agreement with what we found in the experiments.

We performed natural population analysis to investigate the charge distributions and charge transfer of the most stable isomers of  $\text{TiAlO}_y^-$  ( $y=1-3$ ) and  $\text{TiAl}_2\text{O}_y^-$  ( $y=2-3$ ) clusters and their corresponding neutrals. The natural populations and natural electron configurations of isomers 4A and 4B are very close. Thus, only those of isomer 4A are listed. The natural electron configurations of the valence orbitals and natural charges are compiled in Table III. The small populations of the extra-valence-shell orbitals, such as  $\text{O}(3s3p)$ ,  $\text{Al}(4s3d)$ , and  $\text{Ti}(4p)$  are ignored.

From Table III, we can see that the Ti atom forms bond(s) with the O atoms mainly by contributing the  $4s$  electrons to the O atoms. The Al atoms mainly donate the  $3p$  electrons plus a little contribution from its  $3s$  electrons. In  $\text{TiAlO}$  neutral, the Al atom has more positive charge than the Ti atom. This situation is reversed when more oxygen atoms are involved. In  $\text{TiAlO}_{2,3}$  cluster, the Ti atom is more positively charged than the Al atoms. The natural population analysis of  $\text{TiAlO}_y$  neutral indicates that the positive charge on Ti atom increases from 0.74 to 1.73 e when the number of O atom increases from 1 to 3. That means the Ti atom takes more part in the sequential oxidation. The Al–O bond (1.71 Å) of  $\text{TiAlO}$  (Fig. 4, 1A') is slightly shorter than its Ti–O bond (1.85 Å); while the Al–O bonds (1.95 Å) in  $\text{TiAlO}_2$  (Fig. 4, 2A') are longer than the Ti–O bonds (1.72 Å). Thus, the order of the bond lengths is consistent with the order of charge distributions on the Ti and Al atoms. Similar to that in the  $\text{TiAlO}_y$  clusters, for  $\text{TiAl}_2\text{O}_y$ , the positive charge on the Ti atom also increase from 1.28 to 1.79 e as the number of oxygen atoms increases from 2 to 3.

## V. CONCLUSIONS

We measured the photoelectron spectra of small titanium-aluminum oxide clusters,  $\text{TiAlO}_y^-$  ( $y=1-3$ ) and  $\text{TiAl}_2\text{O}_y^-$  ( $y=2-3$ ), and investigated the structures of these clusters and their corresponding neutrals with density functional calculations. By comparing the theoretical calculated ADEs and VDEs with the experimental measurements, we tentatively determined the structures of these clusters. The structure of  $\text{TiAlO}^-$  is nearly linear with the O atom in the middle. That of  $\text{TiAlO}_2^-$  is a kite-shaped structure.  $\text{TiAlO}_3^-$  has a kite-shaped  $\text{TiAlO}_2$  unit with the third O atom attaching to the Ti atom.  $\text{TiAl}_2\text{O}_2^-$  has two nearly degenerate Al–O–Ti–O–Al chain structures that can be considered as *cis* and *trans* forms.  $\text{TiAl}_2\text{O}_3^-$  also has two low-lying isomers, kite structure and book structure, coexisting in our experiments. The experiments show that the ADEs of  $\text{TiAlO}_y^-$  and  $\text{TiAl}_2\text{O}_y^-$  (the electron affinities of corresponding neutrals) increase as the number of O atoms increases. The trend of sequential oxidation of Ti and Al in these clusters found by theoretical calculations is consistent with the experimental observation.

## ACKNOWLEDGMENTS

This work was supported by the Natural Science Foundation of China (NSFC, Grant No. 20933008). We are grate-

ful to Professor Zhen Gao and Dr. Xun-Lei Ding for valuable discussions. We thank the Supercomputing Center of Chinese Academy of Sciences for allowing us to use the ScGrid for theoretical calculations.

- <sup>1</sup>X. H. Liu, X. G. Zhang, Y. Li, X. Y. Wang, and N. Q. Lou, *Int. J. Mass Spectrom.* **177**, L1 (1998).
- <sup>2</sup>Y. Matsuda and E. R. Bernstein, *J. Phys. Chem. A* **109**, 314 (2005).
- <sup>3</sup>Y. Gong, Q. Q. Zhang, and M. F. Zhou, *J. Phys. Chem. A* **111**, 3534 (2007).
- <sup>4</sup>I. Garkusha, A. Nagy, Z. Guennoun, and J. P. Maier, *Chem. Phys.* **353**, 115 (2008).
- <sup>5</sup>Y. Gong and M. F. Zhou, *J. Phys. Chem. A* **112**, 9758 (2008).
- <sup>6</sup>H. B. Wu and L. S. Wang, *J. Chem. Phys.* **107**, 8221 (1997).
- <sup>7</sup>H. J. Zhai and L. S. Wang, *J. Am. Chem. Soc.* **129**, 3022 (2007).
- <sup>8</sup>W. Yu and R. B. Freas, *J. Am. Chem. Soc.* **112**, 7126 (1990).
- <sup>9</sup>S. Brünken, H. S. P. Müller, K. M. Menten, M. C. McCarthy, and P. Thaddeus, *Astrophys. J.* **676**, 1367 (2008).
- <sup>10</sup>S. R. Desai, H. B. Wu, and L. S. Wang, *Int. J. Mass Spectrom. Ion Process.* **159**, 75 (1996).
- <sup>11</sup>H. B. Wu, X. Li, X. B. Wang, C. F. Ding, and L. S. Wang, *J. Chem. Phys.* **109**, 449 (1998).
- <sup>12</sup>S. R. Desai, H. B. Wu, C. M. Rohlfing, and L. S. Wang, *J. Chem. Phys.* **106**, 1309 (1997).
- <sup>13</sup>M. Sierka, J. Dobler, J. Sauer, H. J. Zhai, and L. S. Wang, *ChemPhys-Schem* **10**, 2410 (2009).
- <sup>14</sup>F. A. Akin and C. C. Jarrold, *J. Chem. Phys.* **118**, 5841 (2003).
- <sup>15</sup>F. A. Akin and C. C. Jarrold, *J. Chem. Phys.* **118**, 1773 (2003).
- <sup>16</sup>G. Meloni, M. J. Ferguson, and D. M. Neumark, *Phys. Chem. Chem. Phys.* **5**, 4073 (2003).
- <sup>17</sup>S. M. Sonchik, L. Andrews, and K. D. Carlson, *J. Phys. Chem.* **87**, 2004 (1983).
- <sup>18</sup>S. J. Bares, M. Haak, and J. W. Nibler, *J. Chem. Phys.* **82**, 670 (1985).
- <sup>19</sup>L. Andrews, T. R. Burkholder, and J. T. Yustein, *J. Phys. Chem.* **96**, 10182 (1992).
- <sup>20</sup>G. Santambrogio, E. Janssens, S. H. Li, T. Siebert, G. Meijer, K. R. Asmis, J. Dobler, M. Sierka, and J. Sauer, *J. Am. Chem. Soc.* **130**, 15143 (2008).
- <sup>21</sup>K. Demyk, D. van Heijnsbergen, G. von Helden, and G. Meijer, *Astron. Astrophys.* **420**, 547 (2004).
- <sup>22</sup>A. Hagfeldt, R. Bergstrom, H. O. G. Siegbahn, and S. Lunell, *J. Phys. Chem.* **97**, 12725 (1993).
- <sup>23</sup>A. Hagfeldt, S. Lunell, and H. O. G. Siegbahn, *Int. J. Quantum Chem.* **49**, 97 (1994).
- <sup>24</sup>C. Sousa and F. Illas, *Phys. Rev. B* **50**, 13974 (1994).
- <sup>25</sup>R. Bergström, S. Lunell, and L. A. Eriksson, *Int. J. Quantum Chem.* **59**, 427 (1996).
- <sup>26</sup>T. Albaret, F. Finocchi, and C. Noguera, *Appl. Surf. Sci.* **144-145**, 672 (1999).
- <sup>27</sup>M. B. Walsh, R. A. King, and H. F. Schaefer, *J. Chem. Phys.* **110**, 5224 (1999).
- <sup>28</sup>T. Albaret, F. Finocchi, and C. Noguera, *J. Chem. Phys.* **113**, 2238 (2000).
- <sup>29</sup>G. L. Gutsev, B. K. Rao, and P. Jena, *J. Phys. Chem. A* **104**, 11961 (2000).
- <sup>30</sup>K. S. Jeong, C. Chang, E. Sedlmayr, and D. Sulzle, *J. Phys. B* **33**, 3417 (2000).
- <sup>31</sup>Z. W. Qu and G. J. Kroes, *J. Phys. Chem. B* **110**, 8998 (2006).
- <sup>32</sup>F. Grein, *J. Chem. Phys.* **126**, 034313 (2007).
- <sup>33</sup>Z. W. Qu and G. J. Kroes, *J. Phys. Chem. C* **111**, 16808 (2007).
- <sup>34</sup>S. G. Li and D. A. Dixon, *J. Phys. Chem. A* **112**, 6646 (2008).
- <sup>35</sup>Z. H. Lu and J. X. Cao, *Chin. Phys. B* **17**, 3336 (2008).
- <sup>36</sup>E. L. Uzunova, H. Mikosch, and G. S. Nikolov, *J. Chem. Phys.* **128**, 094307 (2008).
- <sup>37</sup>Y. Z. Liu, Y. B. Yuan, Z. B. Wang, K. M. Deng, C. Y. Xiao, and Q. X. Li, *J. Chem. Phys.* **130**, 174308 (2009).
- <sup>38</sup>B. H. Lengsfeld and B. Liu, *J. Chem. Phys.* **77**, 6083 (1982).
- <sup>39</sup>J. Rubio, J. M. Ricart, and F. Illas, *J. Comput. Chem.* **9**, 836 (1988).
- <sup>40</sup>A. Márquez, M. J. Capitán, J. A. Odriozola, and J. F. Sanz, *Int. J. Quantum Chem.* **52**, 1329 (1994).
- <sup>41</sup>J. P. Towle, A. M. James, O. L. Bourne, and B. Simard, *J. Mol. Spectrosc.* **163**, 300 (1994).
- <sup>42</sup>T. K. Ghanty and E. R. Davidson, *J. Phys. Chem. A* **103**, 8985 (1999).

- <sup>43</sup>T. K. Ghanty and E. R. Davidson, *J. Phys. Chem. A* **103**, 2867 (1999).
- <sup>44</sup>A. Martínez, F. J. Tenorio, and J. V. Ortiz, *J. Phys. Chem. A* **105**, 11291 (2001).
- <sup>45</sup>A. Martínez, F. J. Tenorio, and J. V. Ortiz, *J. Phys. Chem. A* **105**, 8787 (2001).
- <sup>46</sup>X. Y. Cui, I. Morrison, and J. G. Han, *J. Chem. Phys.* **117**, 1077 (2002).
- <sup>47</sup>A. Martínez, L. E. Sansores, R. Salcedo, F. J. Tenorio, and J. V. Ortiz, *J. Phys. Chem. A* **106**, 10630 (2002).
- <sup>48</sup>A. Martínez, F. J. Tenorio, and J. V. Ortiz, *J. Phys. Chem. A* **107**, 2589 (2003).
- <sup>49</sup>A. B. C. Patzer, C. Chang, E. Sedlmayr, and D. Sulzle, *Eur. Phys. J. D* **32**, 329 (2005).
- <sup>50</sup>S. Neukermans, N. Veldeman, E. Janssens, P. Lievens, Z. Chen, and P. V. R. Schleyer, *Eur. Phys. J. D* **45**, 301 (2007).
- <sup>51</sup>J. Sun, W. C. Lu, H. Wang, L. Z. Zhao, Z. S. Li, and C. C. Sun, *Int. J. Quantum Chem.* **107**, 1915 (2007).
- <sup>52</sup>E. F. Archibong, N. Seeburrun, and P. Ramasami, *Chem. Phys. Lett.* **481**, 169 (2009).
- <sup>53</sup>L. G. Wang and M. M. Kukulja, *J. Phys. Chem. Solids* **71**, 140 (2010).
- <sup>54</sup>N. V. Nguyen, J.-P. Han, J. Y. Kim, E. Wilcox, Y. J. Cho, W. Zhu, Z. Luo, and T. P. Ma, *AIP Conf. Proc.* **683**, 181 (2003).
- <sup>55</sup>O. Auciello, W. Fan, B. Kabius, S. Saha, J. A. Carlisle, R. P. H. Chang, C. Lopez, E. A. Irene, and R. A. Baragiola, *Appl. Phys. Lett.* **86**, 042904 (2005).
- <sup>56</sup>S. J. Yun, J. S. Noh, and J. W. Lim, ECS Meeting Abstracts, 2009, Vol. 902, p. 765.
- <sup>57</sup>A. Tamanai, H. Mutschke, J. Blum, T. Posch, C. Koike, and J. W. Ferguson, *Astron. Astrophys.* **501**, 251 (2009).
- <sup>58</sup>O. Cheshnovsky, S. H. Yang, C. L. Pettiette, M. J. Craycraft, and R. E. Smalley, *Rev. Sci. Instrum.* **58**, 2131 (1987).
- <sup>59</sup>H.-G. Xu, Z.-G. Zhang, Y. Feng, J. Y. Yuan, Y. C. Zhao, and W. J. Zheng, *Chem. Phys. Lett.* **487**, 204 (2010).
- <sup>60</sup>M. J. Frisch, G. W. Trucks, H. B. Schlegel *et al.*, GAUSSIAN 03, Gaussian, Inc., Pittsburgh, PA, 2003.
- <sup>61</sup>A. D. Becke, *J. Chem. Phys.* **98**, 5648 (1993).
- <sup>62</sup>C. Lee, W. Yang, and R. G. Parr, *Phys. Rev. B* **37**, 785 (1988).
- <sup>63</sup>K. P. Huber and G. Herzberg, *Constants of Diatomic Molecules* (Van Nostrand Reinhold, New York, 1979).
- <sup>64</sup>E. D. Glendenning, A. E. Reed, J. E. Carpenter, and F. Weinhold, NBO Version 3.1.
- <sup>65</sup>A. V. Nemukhin and F. Weinhold, *J. Chem. Phys.* **97**, 3420 (1992).
- <sup>66</sup>J. B. Pedley and E. M. Marshall, *J. Phys. Chem. Ref. Data* **12**, 967 (1983).